Thermochimica Acta, 164 (1990) 365–378
Elsevier Science Publishers B.V., Amsterdam

THERMAL INVESTIGATION AND STEREOCHEMICAL STUDIES OF SOME CYCLIC LIGAND COMPLEXES OF NICKEL(II) AND ZINC(II) IN THE SOLID STATE

RAJKUMAR BHUBON SINGH and SAMIRAN MITRA *

Department of Chemistry, Manipur University, Canchipur Imphal 795003 (India)

(Received 18 December 1989)

ABSTRACT

1,4-Morpholine (morph) and 1,4-thioxane (thiox) complexes of nickel(II) and zinc(II) were synthesized. A thermal investigation was carried out and the stereochemical changes which occured during thermal decomposition were studied. The complexes were found to have the compositions $[NiCl_2(morph)(H_2O)_2]$, $[NiBr_2(morph)(H_2O)_2]$, $[Ni(SCN)_2(morph)_2]$, $[ZnCl_2(morph)]$, $[ZnBr_2(morph)_2]$, $[Zn(SCN)_2(morph)_2]\cdot 2H_2O$, $[ZnCl_2(thiox)]$, $[ZnBr_2(thiox)]\cdot 2H_2O$ and $[Zn(SCN)_2(thiox)]$. Attempts to prepare thioxane complexes of Ni^{II} and dithiane complexes of Ni^{II} and Zn^{II} failed. The characterization and study of configurational and conformational changes were studied with the help of elemental and thermal analyses, IR, far-IR, magnetic moment and conductivity measurements. The morpholine complexes of nickel(II) and zinc(II) appeared to be octahedral except $[ZnCl_2(morph)]$, which is tetrahedral, and thioxane complexes of zinc(II) appeared to be tetrahedral. Thermodynamic parameters, such as activation energy $E_a^\star$, enthalpy change ΔH and entropy change ΔS, were evaluated for the dehydration steps and decomposition reactions of the complexes using some standard methods. A linear correlation was found between $E_a^\star$ and ΔS for the decomposition reactions of the complexes.

INTRODUCTION

Acyclic ligands having oxygen, sulphur or nitrogen donor atoms in their structures can be the best chelating agents for transition and non-transition metal ions [1–3]. However, works on cyclic ligand complexes are still very scarce [4–11], and there has been little thermal investigation of cyclic ligand complexes in the solid state [12–15]. The main aim of the present work is to synthesize some cyclic ligand (six-membered ring) complexes of nickel(II) and zinc(II) and to study the stereochemical changes during thermal decomposition. The purpose of selecting the above-mentioned cyclic ligands was also to see the effect on stability of the complexes where these are formed

---

* Author to whom correspondence should be addressed.

0040-6031/90/$03.50

via two different donor centres in the same molecule, but it has not been possible to draw any definite conclusion on this.

Prior to heating, the cyclic ligands morpholine and thioxane function as bidentate chelating agents (boat form) [12] in all the complexes, as shown by the increased number of IR bands in the range 700–1300 cm^{-1} compared with those observed for the free ligand (chair form) [9–16]. If these complexes are heated under non-isothermal conditions they decompose via intermediates (stable or unstable) in which the cyclic ligand functions as a bidentate chelate (boat form) or a bridging bidentate chelate (chair form). This kind of conformational change of the ligand (boat → chair) has been confirmed by IR and far-IR data. Chloride, bromide and thiocyanate ions in these complexes might occur as terminal unidentate ligands or, in some cases, as a bridging bidentate ligand [17]. Parameters such as $E_a^\star$, ΔH and ΔS have been evaluated for the dehydration step and decomposition reactions of the complexes in the solid state.

EXPERIMENTAL

Materials and methods

Metal chlorides were of AnalaR grade and were used as received. Metal bromides were freshly prepared by neutralizing a concentrated hydrobromic acid (AnalaR grade) solution with the corresponding metal carbonate (AnalaR grade), filtering and subsequently crystallizing out the required bromide from the filtrate obtained. Metal thiocyanates were freshly prepared by mixing an ethanolic solution of the metal salt with potassium thiocyanate, filtering and subsequently crystallizing out the required thiocyanate from the filtrate obtained.

Morpholine (E. Merck, India) and thioxane (Aldrich Co., U.S.A.) were used as received. Ethanol and diethyl ether were dried using standard procedures [18].

Preparation of the complexes

For $[NiCl_2(morph)(H_2O)_2]$ (**1a**), the ligand (ca. 7 mmol) dissolved in dry ethanol (40 cm^3) was added with constant stirring to a dry ethanolic solution (50 cm^3) containing nickel chloride (ca. 4 mmol). The bluish nickel complex was collected by filtration, washed carefully with dry diethyl ether and dried over fused calcium chloride in a desiccator. Yield ca. 80%.

The complexes $[NiBr_2(morph)(H_2O)_2]$ (**2a**), $[Ni(SCN)_2(morph)_2]$ (**3a**), $[ZnCl_2(morph)]$ (**4a**), $[ZnBr_2(morph)_2]$ (**5a**), $[Zn(SCN)_2(morph)_2] \cdot 2H_2O$ (**6a**), $[ZnCl_2(thiox)]$ (**7a**), $[ZnBr_2(thiox)] \cdot 2H_2O$ (**8a**) and $[Zn(SCN)_2(thiox)]$ (**9a**) were prepared similarly.

Elemental analyses, thermal study, IR spectra, magnetic moment, conductivity measurements

Nickel and zinc were estimated gravimetrically using standard procedures [19], and carbon, hydrogen and nitrogen were determined using a Carlo Erba 1106 elemental analyser. Results of elemental analyses are given in Table 1. Thermal investigations (TG and DTA) were carried out on a Shimadzu DT-30 thermal analyser under a dynamic nitrogen atmosphere with a heating rate of 10 °C min^{-1}. α-alumina was used as a standard. The activation energy $E_a^\star$ was computed from the TG curve using the equation of Horowitz and Metzger [20] and from the DTA curve using that of Borchardt and Daniels [21]. The enthalpy change ΔH was evaluated from the DTA curve using the relation $\Delta H = KA$, where K is the heat-transfer coefficient (the calibration or cell constant; the cell used was a platinum crucible and its constant K was evaluated from the data obtained using indium metal as a calibrant) and A is the total area under the particular DTA peak measured using a compensating planimeter with the optical tracer Fuji Corona 027. The entropy change ΔS was calculated using the relation [22] $\Delta S = \Delta H/T_m$, where T_m is the DTA peak temperature in K. IR and far-IR spectra were recorded using Perkin–Elmer 284, 363, 597 and 783 models in KBr, CsCl or polythene discs. The effective magnetic moments were evaluated from the results of magnetic susceptibility measurements using an EG and G PAR 155 vibrating sample magnetometer. Conductances were measured using a Systrons (India) conductivity bridge, model no. 304.

RESULTS AND DISCUSSION

*[NiCl$_2$(morph)(H$_2$O)$_2$] (**1a**) and [NiBr$_2$(morph)(H$_2$O)$_2$] (**2a**)*

The bluish green complexes have not been reported previously. The presence of coordinated water molecules is confirmed by the appearance of IR bands [12,13,17] at 3380 and 3360 cm^{-1} [ν(OH)], 1640, 1630 and 1623 cm^{-1} [δ(HOH)] and 446, 430 and 390 cm^{-1} [ν(Ni–O)] in [Ni–OH$_2$], and 547 and 490 cm^{-1} [$\rho_\omega(H_2O)$] (Tables 2 and 3). Furthermore, the weight loss in the TG curves of **1a** and **2a** in the ranges 85–125 °C and 40–145 °C and endothermic peaks in the DTA curves at 123 °C and 140 °C (Fig. 1) correspond to two molecules of water. The anhydrous complex [NiCl$_2$(morph)] decomposes to $NiCl_2$ via the formation of [NiCl$_2$(morph)$_{0.5}$] (**1c**) in the ranges 126–199 °C and 199–280 °C. The complex [NiBr$_2$(morph)] decomposes to $NiBr_2$ in a single step (Table 4 and Fig. 1). The corresponding DTA curve shows endothermic peaks at 192, 243 and 250 °C. The intermediate complex **1c** was isolable at around 200 °C by holding the heating rate at 0.5 °C min^{-1}. Values of $E_a^\star$, ΔH and ΔS for the conversions

TABLE 1

Analytical data (calculated values in parentheses) and effective magnetic moment data of morpholine (morph) and thioxane (thiox) complexes of Ni^{II} and Zn^{II}

No.	Complex	Colour	Analysis (%)				μ_{eff} (B.M.)
			Metal	Carbon	Hydrogen	Nitrogen	
1a	$[NiCl_2(morph)(H_2O)_2]$	Bluish green	23.29 (23.23)	18.90 (18.99)	5.16 (5.14)	5.41 (5.54)	2.81
2a	$[NiBr_2(morph)(H_2O)_2]$	Bluish green	17.00 (17.18)	14.00 (14.04)	3.92 (3.89)	4.00 (4.09)	2.67
3a	$[Ni(SCN)_2(morph)_2]$	Blue	16.75 (16.83)	34.37 (34.41)	5.06 (5.16)	15.95 (16.06)	2.38
3b	$[Ni(SCN)_2(morph)]$	Light chocolate	22.49 (22.43)	27.37 (27.51)	3.30 (3.44)	16.00 (16.05)	2.23
4a	$[ZnCl_2(morph)]$	White	29.16 (29.24)	21.40 (21.49)	3.90 (4.03)	6.12 (6.26)	
5a	$[ZnBr_2(morph)_2]$	Cream	16.30 (16.35)	24.05 (24.04)	4.48 (4.50)	6.91 (7.01)	
6a	$[Zn(SCN)_2(morph)_2]\cdot 2H_2O$	Cream	16.69 (16.66)	30.69 (30.66)	5.48 (5.62)	14.25 (14.31)	
7a	$[ZnCl_2(thiox)]$	White	27.19 (27.17)	19.89 (19.97)	3.27 (3.33)	–	
8a	$[ZnBr_2(thiox)]\cdot 2H_2O$	White	17.82 (17.87)	13.29 (13.13)	3.25 (3.28)	–	
9a	$[Zn(SCN)_2(thiox)]$	White	22.90 (22.89)	25.15 (25.23)	2.71 (2.80)	–	

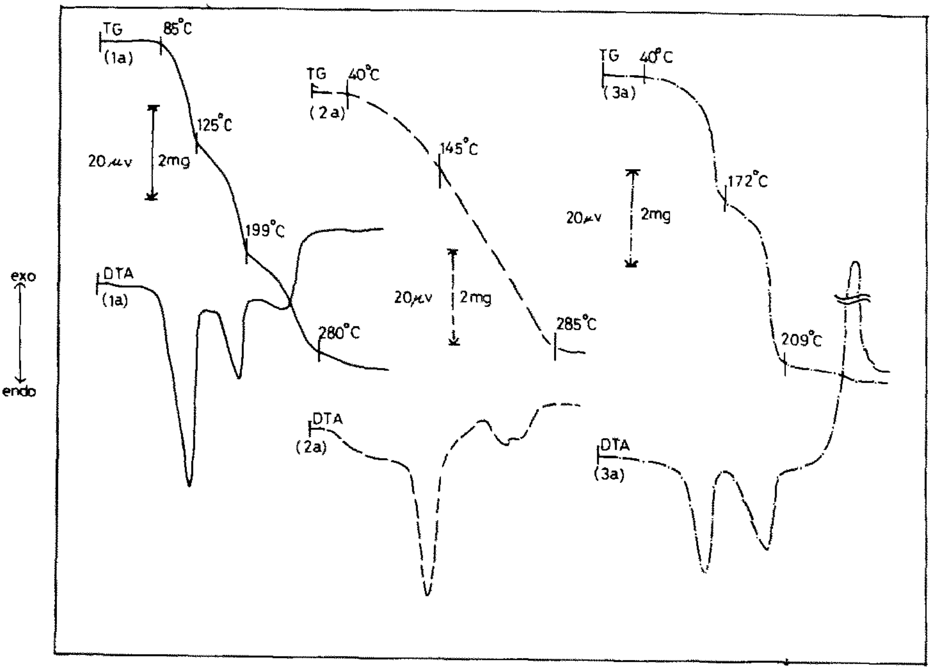

Fig. 1. Thermal curves: ——, $[NiCl_2(morph)(H_2O)_2]$ (**1a**), sample mass 13.4 mg; — — —, $[NiBr_2(morph)(H_2O)_2]$ (**2a**), sample mass 14.3 mg; ·—·—·, $[Ni(SCN)_2(morph)_2]$ (**3a**), sample mass 12.1 mg.

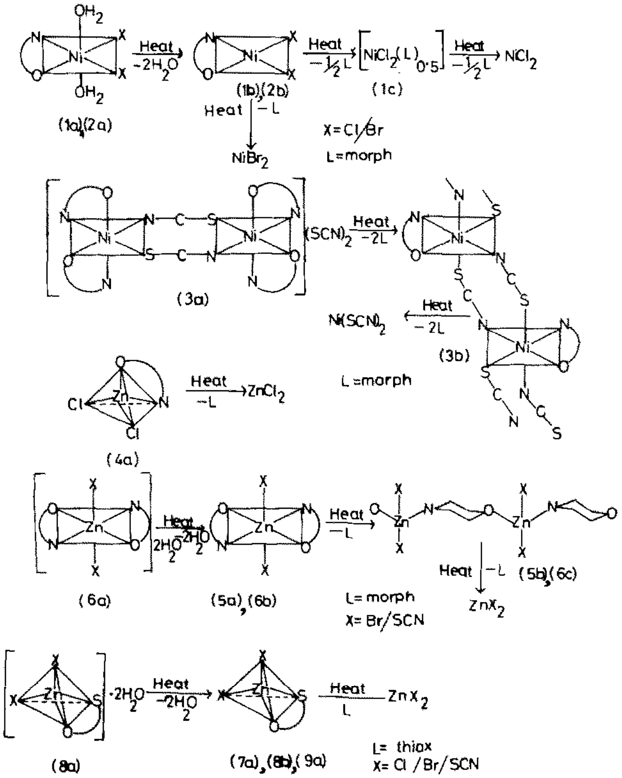

Scheme 1. Probable reaction pathways.

TABLE 2

IR spectral data (cm^{-1}) for Ni^{II} and Zn^{II} cyclic ligand complexes

No.	Complex [a]	IR spectral data [b]											
		ν(OH)	δ(HOH)	ρ_r(HOH)	ρ_w(HOH)	ν(NH)	ν_a(COC)	ν_s(COC)	ν(CSC)	ν(CN)	ν(CS)	δ(NCS)	Other bands
1a	[NiCl$_2$L(H$_2$O)$_2$]	3380 (s) 3360 (br)	1640 (ms) 1630 (sh) 1623 (s)	858 (vw)	547 (w) 490 (s) 485 (sh)	3249 (s) 3240 (ms) 3215 (w)	1080 (s) 1078 (sh) 1048 (s) 1041 (w)	831 (s) 822 (w)	–	–	–	–	1295 (w), 1250 (ms) 1225 (s), 1216 (w) 1190 (sh), 1178 (w) 1035 (vs), 1025 (sh) 1010 (sh), 996 (vs) 899 (vs), 876 (s) 750 (w), 725 (s)
1b	[NiCl$_2$(L)$_{0.5}$]	–	–	–	–	3280 (w) 3040 (br)	1040 (vs)	820 (vw)	–	–	–	–	1290 (sh), 1220 (s) 1210 (sh), 1185 (s) 1150 (w), 1140 (w) 1095 (vs), 1110 (sh) 895 (vs), 870 (sh) 867 (vs)
2a	[NiBr$_2$L(H$_2$O)$_2$]	3420 (s)	1630 (s) 1615 (w)	818 (vs)	485 (s) 470 (w) 465 (w) 440 (s)	3280 (sh) 3220 (s)	1080 (s) 1049 (s) 1030 (ms)	830 (s) 825 (sh)	–	–	–	–	1295 (sh), 1255 (w) 1225 (s), 1220 (sh) 1188 (ms), 1174 (w) 1040 (w), 1035 (sh) 900 (sh), 895 (vs) 875 (ms), 750 (sh) 760 (w), 755 (s)
3a	[Ni(SCN)$_2$L$_2$]	–	–	–	–	3220 (s)	1080 (s) 1045 (s) 1025 (s)	830 (w) 825 (w)	–	2120 (vs) 2075 (w)	840 (s) 825 (ms) 785 (w)	480 (s) 448 (sh) 435 (w) 425 (w)	1252 (vs), 1200 (s) 1172 (ms), 1115 (vs) 1030 (w), 1022 (sh) 1015 (vs), 1000 (vs) 960 (w), 935 (vw) 899 (vs), 880 (vs) 785 (ms), 755 (w)
3b	[Ni(SCN)$_2$L]	–	–	–	–	3220 (s)	1045 (s) 1025 (s)	830 (w) 825 (w)	–	2109 (vs) 2070 (sh)	830 (w) 825 (sh) 785 (w)	480 (s) 470 (w)	1300 (sh), 1250 (s) 1198 (w), 1170 (s) 1113 (vs), 1020 (sh) 995 (vs), 890 (ms) 880 (vs), 750 (s)
4a	[ZnCl$_2$L]	–	–	–	–	3255 (s)	1078 (s) 1068 (ms) 1045 (w)	832 (s) 816 (ms)	–	–	–	–	1300 (vs), 1255 (ms), 1230 (vw) 1190 (w), 1040 (vw),

												1030 (w) 1007 (w), 970 (w) 952 (sh) 940 (vs), 900 (w), 855 (s) 800 (w), 745 (w)
5a	[$ZnBr_2L_2$]	–	–	–	–	3198 (s) 3130 (s)	1078 (s) 1068 (vs) 1031 (s)	835 (w)	–	–	–	–	1292 (vs), 1255 (vs), 1204 (ms) 1187 (sh), 1185 (s), 1121 (s) 1119 (sh), 1041 (vw), 1024 (s) 1005 (s), 964 (ms), 895 (sh) 885 (s), 878 (sh), 825 (s) 815 (sh), 772 (w), 735 (w)
6a	[$Zn(SCN)_2L_2$] $\cdot 2H_2O$	3460 (br) 3450 (w)	1649 (w) 1642 (w)	–	–	3235 (vs) 3204 (ms)	1078 (ms) 1064 (vs) 1041 (ms)	835 (ms) 832 (sh) 825 (s)	–	2050 (s) 2045 (sh)	835 (ms) 825 (s)	484 (ms)	1300 (w), 1260 (vs), 1224 (s) 1198 (ms), 1115 (vs), 1100 (w), 1058 (w), 1030 (s), 1015 (sh) 897 (s), 884 (s), 878 (ms) 850 (s)
7a	[$ZnCl_2L'$]	–	–	–	–	–	1057 (s) 1050 (ms)	828 (ms) 820 (s)	655 (s)	–	–	–	1251 (vs), 1200 (s), 1172 (w) 1000 (vs), 960 (vw), 952 (sh) 880 (vs), 860 (s), 836 (w) 785 (s, br), 742 (w)
8a	[$ZnBr_2L'$] $\cdot 2H_2O$	3430 (w) 3415 (w)	1642 (w) 1632 (br)	–	–	–	1056 (s) 1047 (sh) 1030 (ms)	829 (ms) 817 (sh) 809 (s)	660 (w) 652 (ms)	–	–	–	1290 (w), 1243 (s), 1180 (w) 1160 (s), 1153 (w), 1110 (vs) 1062 (vw), 1025 (s), 1011 (w) 1005 (vw), 952 (vs), 890 (sh) 881 (vs)

TABLE 2 (continued)

No.	Complex [a]	IR spectral data [b]											
		ν(OH)	δ(HOH)	ρ_r(HOH)	ρ_w(HOH)	ν(NH)	ν_a(COC)	ν_s(COC)	ν(CSC)	ν(CN)	ν(CS)	δ(NCS)	Other bands
9a	$[Zn(SCN)_2L']$	–	–	–	–	–	1050 (s) 1040 (sh) 1035 (ms)	832 (w) 827 (s) 820 (ms)	663 (s) 657 (ms)	2060 (s) 2051 (w)	744 (ms) 731 (w)	480 (s)	1225 (vs), 1189 (s), 1027 (vw) 1009 (vw), 895 (vs), 880 (ms) 860 (s), 842 (vw), 802 (vw) 782 (s), 755 (vw), 720 (w)

---

[a] L, morpholine; L′, thioxane. [b] vs, Very strong; ms, medium strong; s, strong; sh, shoulder; w, weak; vw, very weak; br, broad. In some complexes containing thiocyanate ions, bands for ν(CS) overlapped with the ν_s(COC) bands of some cyclic ligands.

TABLE 3

Far-IR spectral data [a] (cm^{-1}) for Ni^{II} and Zn^{II} cyclic ligand complexes

No.	Complex [b]	Far-IR data [c]				
		ν(M–O)	ν(M–N)	ν(M–S)	ν(M–X) [d]	∂(M–X)
1a	$[NiCl_2L(H_2O)_2]$	446 (s) 430 (ms) 390 (w)	340 (w) 331 (s)	–	297 (s) 290 (sh)	135 (w)
2a	$[NiBr_2L(H_2O)_2]$	472 (s) 460 (s)	310 (s) 295 (w)	–	280 (w) 260 (s) 251 (s)	175 (s) 150 (w)
3a	$[Ni(SCN)_2L_2]$	430 (s) 380 (w)	344 (vs)	–	–	–
3b	$[Ni(SCN)_2L]$	455 (s) 415 (w)	340 (vs) 321 (w)	–	–	–
4a	$[ZnCl_2L]$	450 (ms) 420 (w)	352 (ms)	–	326 (w) 312 (s)	137 (w) 120 (s)
5a	$[ZnBr_2L_2]$	464 (ms) 444 (w)	321 (ms)	–	252 (ms) 224 (w)	–
6a	$[Zn(SCN)_2L_2]\cdot 2H_2O$	444 (ms)	370 (ms) 340 (ms) 303 (ms)	–	–	–
7a	$[ZnCl_2L']$	525 (s)	–	340 (w) 327 (w)	310 (s) 300 (ms)	–
8a	$[ZnBr_2L']\cdot 2H_2O$	459 (s) 437 (w)	–	330 (s) 312 (w)	289 (ms) 271 (sh)	–
9a	$[Zn(SCN)_2L']$	460 (ms) 442 (w)	–	345 (ms) 320 (w)	–	–

---

[a] For cyclic ligands (morpholine and thioxane) and coordinated water molecules, bands for ν(M–O) overlapped with one other.

[b] L, Morpholine; L′, thioxane.

[c] s, Strong; ms, medium strong; vs, very strong; sh, shoulder; w, weak; vw, very weak.

[d] X ≡ Cl or Br.

of **1a** → **1b**, **1b** → **1c**, **1c** → $NiCl_2$ and **2a** → **2b**, **2b** → $NiBr_2$ are given in Table 4. The bluish green colour and the values of the effective magnetic moments ($\mu_{eff} = 2.81$ and 2.67 B.M. for **1a** and **2a** respectively) suggest an octahedral structure. In these complexes the cyclic ligand (morph) functions as a bidentate chelating agent in the boat form [12], as shown by the greater number of IR spectral bands in the 700–1300 cm^{-1} region (Table 2) compared with those for the free ligand which exists in the chair form [5,9,16]. The probable path of decomposition of **1a** and **2a** are shown in Scheme 1.

$[Ni(SCN)_2(morph)_2]$ (3a)

This complex has not been reported previously. On heating, **3a** undergoes decomposition into $Ni(SCN)_2$ via the intermediate $[Ni(SCN)_2(morph)]$ in

TABLE 4

Thermal parameters of morpholine (morph) and thioxane (thiox) complexes of Ni^{II} and Zn^{II}

No.	Decomposition reactions	TG temp. range (°C)	DTA peak temp (°C)		$E_a^\star$ (kJ mol^{-1})		Enthalpy change ΔH (kJ mol^{-1})	Entropy change ΔS (J K^{-1} mol^{-1})
			Endo	Exo	TG	DTA		
1 (a)	$[NiCl_2(morph)(H_2O)_2] \rightarrow [NiCl_2(morph)]$	85–125	123	–	76.82	134.50	91.36	232.46
(b)	$[NiCl_2(morph)] \rightarrow [NiCl_2(morph)_{0.5}]$	126–199	192	–	71.23	169.74	27.16	58.41
(c)	$[NiCl_2(morph)_{0.5}] \rightarrow NiCl_2$	199–280	243	–	89.12	155.82	16.46	31.90
2 (a)	$[NiBr_2(morph)(H_2O)_2] \rightarrow [NiBr_2(morph)]$	40–145	140	–	21.38	144.96	58.56	141.78
(b)	$[NiBr_2(morph)] \rightarrow NiBr_2$	145–235	250	–	32.69	86.25	31.23	59.71
3 (a)	$[Ni(SCN)_2(morph)_2] \rightarrow [Ni(SCN)_2(morph)]$	40–172	125	–	44.05	57.85	58.15	146.12
(b)	$[Ni(SCN)_2(morph)] \rightarrow Ni(SCN)_2$	173–209	205	–	218.25	21.30	58.03	121.40
4 (a)	$[ZnCl_2(morph)] \rightarrow ZnCl_2$	42–305	95 [a] 149 209	–	14.01	24.93	27.52	74.79
5 (a)	$[ZnBr_2(morph)_2] \rightarrow [ZnBr_2(morph)]$	177–280	227	–	59.28	68.42	111.70	223.41
(b)	$[ZnBr_2(morph)] \rightarrow ZnBr_2$	280–452	–	312	44.19	75.58	123.19	210.59
6 (a)	$[Zn(SCN)_2(morph)_2] \cdot 2H_2O \rightarrow [Zn(SCN)_2(morph)_2]$	50–172	170	–	18.57	145.20	56.42	127.35
(b)	$[Zn(SCN)_2(morph)_2] \rightarrow [Zn(SCN)_2(morph)]$	173–275	255	–	77.64	178.33	23.84	45.17
(c)	$[Zn(SCN)_2(morph)] \rightarrow Zn(SCN)_2$	275–350	–	295 300 [a]	136.14	156.33	31.65	55.24
7 (a)	$[ZnCl_2(thiox)] \rightarrow ZnCl_2$	57–270	65 130 [a]	–	17.32	20.61	112.38	278.86
8 (a)	$[ZnBr_2(thiox)] \cdot 2H_2O \rightarrow [ZnBr_2(thiox)]$	40–100	96	–	53.26	25.44	91.60	248.24
(b)	$[ZnBr_2(thiox)] \rightarrow ZnBr_2$	100–240	125	–	34.17	127.46	38.29	96.20
9 (a)	$[Zn(SCN)_2(thiox)] \rightarrow Zn(SCN)_2$	110–365	305	–	23.09	74.76	108.02	186.88

[a] Temperature used for the calculation of ΔS.

the ranges 40–172 °C and 173–209 °C (Fig. 1). The corresponding endothermic DTA peaks appear at 125 and 205 °C. Values of E_a^*, ΔH and ΔS for the conversion of **3a** → **3b** and **3b** → $Ni(SCN)_2$ are given in Table 4. Complex **3a** is expected to be dimeric [12] having two thiocyanate ions outside the coordination sphere (see Scheme 1). This is also supported by the molar conductance values [23] ($\Lambda_m = 230\ \Omega^{-1}\ cm^2\ mol^{-1}$ at 25 °C). The intermediate complex **3b** was isolable. The bluish green colour of **3a** and the magnetic moment values of **3a** ($\mu_{eff} = 2.38$ B.M.) and **3b** ($\mu_{eff} = 2.23$ B.M.) indicate that the complexes are octahedral. Complex **3b** is probably polymeric [7,12]; the cyclic ligand functions as a chelate and exists in the boat form while the thiocyanate acts as a bridging bidentate ligand as shown by the bands [5,9,12,17] at 2120, 480 and 448, and 840 and 825 cm^{-1} for ν(CN), δ(NCS) and ν(CS) respectively (Table 2 and Scheme 1).

*[ZnCl$_2$(morph)] (**4a**), [ZnCl$_2$(thiox)] (**7a**), [ZnBr$_2$(thiox)] · 2H$_2$O (**8a**) and [Zn(SCN)$_2$(thiox)] (**9a**)*

Complexes **4a**, **7a** and **8a** have been reported previously [9,24,25]. Our thermal investigation has confirmed that the lattice water of **8a** is lost in the range 40–100 °C in the TG curve; the corresponding DTA curve shows one endothermic peak at 96 °C. Anhydrous complexes **4a**, **7a**, **8b** and **9a** decompose into their metal halides in the ranges 42–305 °C, 57–270 °C, 100–

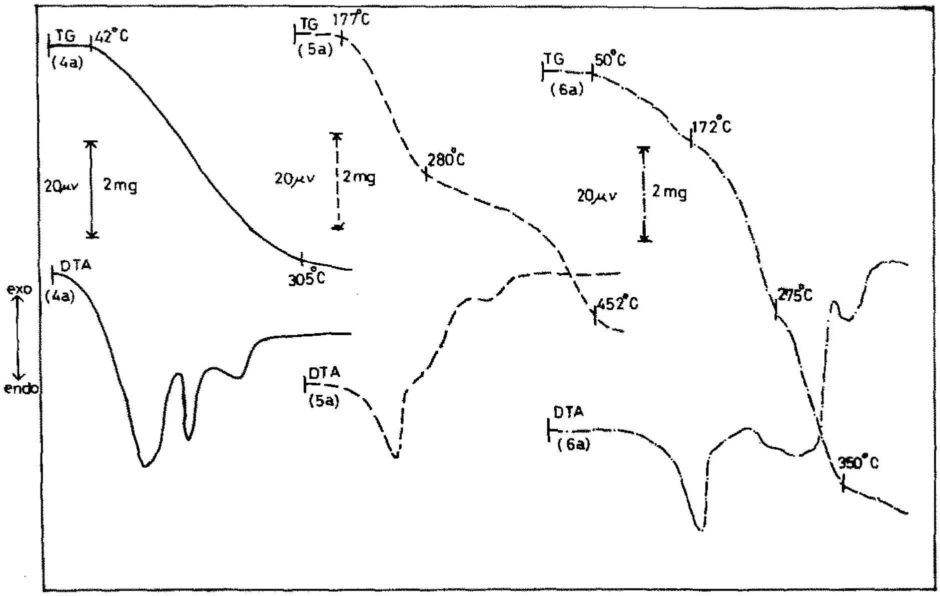

Fig. 2. Thermal curves: ———, [ZnCl$_2$(morph)] (**4a**), sample mass 11.7 mg; — — —, [ZnBr$_2$(morph)$_2$] (**5a**), sample mass 13.4 mg; ·—·—·, [Zn(SCN)$_2$(morph)$_2$]·2H$_2$O (**6a**), sample mass 16.0 mg.

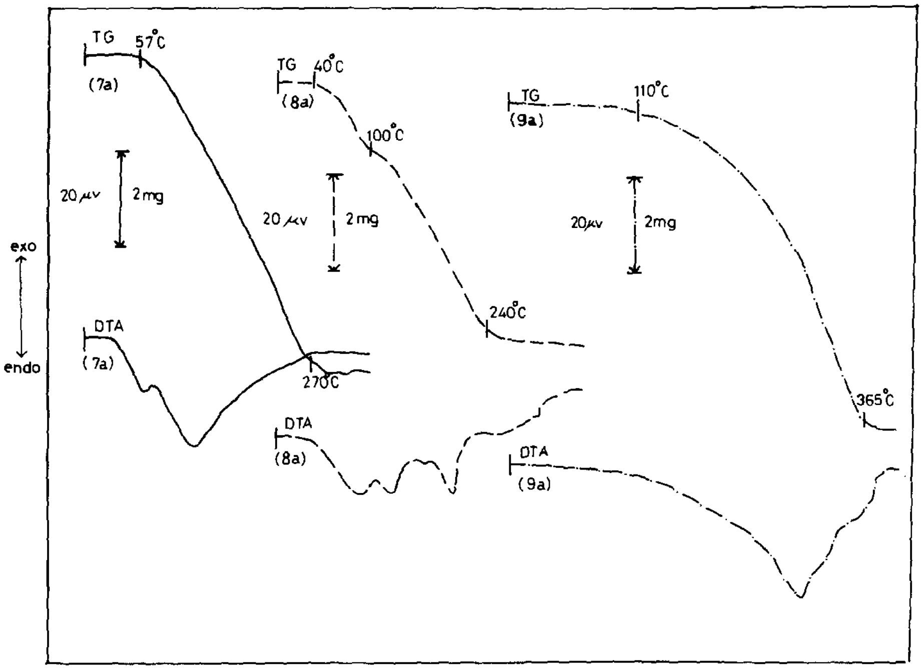

Fig. 3. Thermal curves: ——, [ZnCl$_2$(thiox)] (**7a**), sample mass 14.8 mg; — — —, [ZnBr$_2$(thiox)]·2H$_2$O (**8a**), sample mass 13.8 mg; ·—·—·, [Zn(SCN)$_2$(thiox)] (**9a**), sample mass 17.9 mg.

240 °C and 110–365 °C, as observed in the TG curves; the corresponding DTA peaks appear at 95, 149, 209, 65, 130, 125 and 305 °C (Table 4, Figs. 2 and 3).

In all the complexes **4a**, **7a**, **8a** and **9a**, the cyclic ligands function as bidentate chelating agents and exist in the boat form (Tables 2 and 3). They are expected to have tetrahedral structures. The probable paths of decomposition reactions are given in Scheme 1.

[ZnBr$_2$(morph)$_2$] (5a) and [Zn(SCN)$_2$(morph)$_2$] · 2H$_2$O (6a)

Complex **5a** has been reported previously [24,25]. On pyrolysis, complex **6a** undergoes dehydration to give a complex of the composition [Zn(SCN)$_2$-(morph)$_2$] **6b**. This takes place in the range 50–172 °C (Table 4 and Fig. 2). Complexes **5a** and **6b** decompose into ZnBr$_2$ and Zn(SCN)$_2$ via the formation of the intermediates [ZnBr$_2$(morph)] and [Zn(SCN)$_2$(morph)] **6c**. The ranges for the conversion of **5a** → **5b**, **5b** → ZnBr$_2$, and **6b** → **6c** and **6c** → Zn(SCN)$_2$ are given in Table 4 along with the values of the thermodynamic parameters.

The IR spectra of complexes **5a** and **6a** show that the cyclic ligand which functions as a bidentate chelating agent exists in the boat form (Tables 2

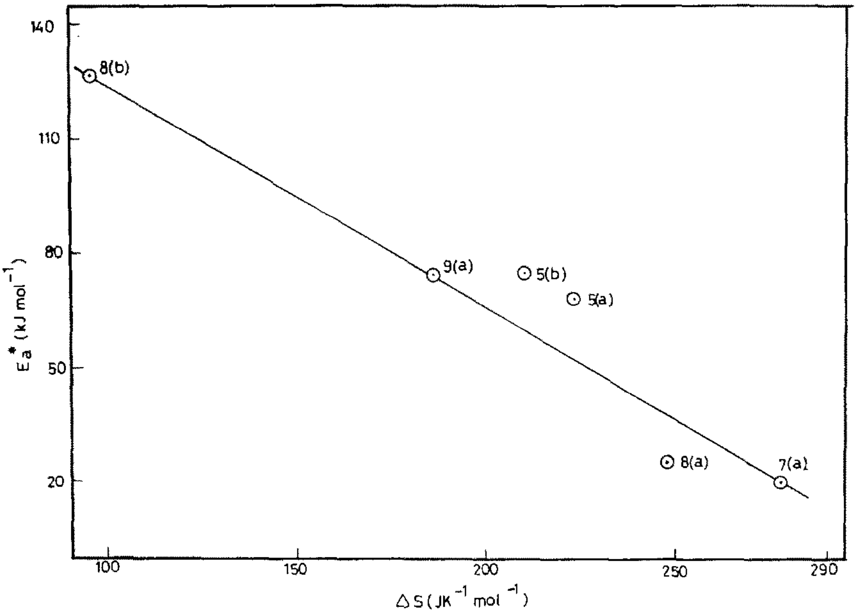

Fig. 4. $E_a^\star$ versus ΔS for the conversions: 5(a), $[ZnBr_2(morph)_2] \rightarrow [ZnBr_2(morph)]$; 5(b), $[ZnBr_2(morph)] \rightarrow ZnBr_2$; 7(a), $[ZnCl_2(thiox)] \rightarrow ZnCl_2$; 8(a), $[ZnBr_2(thiox)] \cdot 2H_2O \rightarrow [ZnBr_2(thiox)]$; 8(b), $ZnBr_2(thiox)] \rightarrow ZnBr_2$; 9(a), $[Zn(SCN)_2(thiox)] \rightarrow Zn(SCN)_2$.

and 3). The bromide and thiocyanate ions act as unidentate ligands [9,17]. These complexes therefore possess an octahedral structure. The probable paths of the dehydration step and the decomposition reaction are given in Scheme 1.

A linear correlation is obtained on plotting $E_a^\star$ versus ΔS. This shows that a system with a higher entropy change ΔS will require less energy $E_a^\star$ for its thermal decomposition [13–15,22] (Fig. 4).

ACKNOWLEDGEMENTS

The authors are grateful to Manipur University for financial assistance (Departmental Fellowship) to R.K.B. Singh. They wish to express their thanks to the Regional Sophisticated Instrumentation Centres at Lucknow and Madras for elemental analyses and IR spectra recording.

REFERENCES

1 R.A. Walton, J. Chem. Soc. A, (1967) 1852.
2 W.K. Musker and M.S. Hussain, Inorg. Chem., 8 (1969) 528.
3 G. De, P.K. Biswas and N. Ray Chaudhuri, J. Chem. Soc., Dalton Trans., (1984) 2581.

4 E.A. Allen, N.P. Johnson, D.T. Rosevear and W. Wilkinson, J. Chem. Soc. A, (1971) 2141.
5 I.S. Ahuja, J. Inorg. Nucl. Chem., 29 (1967) 2091.
6 E.A. Allen, N.P. Johnson, D.T. Rosevear and W. Wilkinson, J. Chem. Soc. A, (1969) 788.
7 P.J. Hendra and D.B. Powell, J. Chem. Soc. A, (1960) 5105.
8 G. Marcotrigiano, L. Menabuea and G.C. Pellacani, J. Chem. Soc., Dalton Trans., (1976) 1627.
9 I.S. Ahuja and R. Singh, J. Coord. Chem., 5 (1976) 167.
10 G.C. Pellacani, R. Battistuzzi and G. Marcotrigiano, J. Inorg. Nucl. Chem., 35 (1973) 2243.
11 K.L. Baker and G.W.A. Fowles, J. Chem. Soc. A, (1968) 801.
12 S. Mitra and L.K. Singh, J. Chem. Soc., Dalton Trans., (1987) 2089.
13 S. Mitra and L.K. Singh, Inorg. Chim. Acta, 133 (1987) 141.
14 S. Mitra and L.K. Singh, Thermochim. Acta, 138 (1989) 285.
15 S. Mitra and L.K. Singh, Thermochim. Acta, 142 (1989) 89.
16 J.D. Donalson and D.G. Nicholson, J. Chem. Soc. A, (1970) 145.
17 K. Nakamoto, Infrared and Raman Spectra of Inorganic and Coordination Compounds, Wiley-Interscience, New York, 3rd edn., 1978, pp. 226, 270 and 322.
18 A.I. Vogel, A Text Book of Practical Organic Chemistry, ELBS and Longman, London, 4th edn., 1980, pp. 269 and 272.
19 A.I. Vogel, A Text Book of Quantitative Inorganic Analysis, ELBS and Longman, London, 3rd edn., 1968, pp. 389, 390 and 480.
20 H.H. Horowitz and G. Metzger, Anal. Chem., 55 (1963) 1414.
21 H.J. Borchardt and F. Daniels, J. Am. Chem. Soc., 79 (1957) 41.
22 R. Roy, M. Chaudhuri, S.K. Mandal and K. Nag, J. Chem. Soc., Dalton Trans., (1984) 1681.
23 S. Glasstone, An Introduction to Electrochemistry, Van Nostrand Company, London, East-West edn., 1965, p. 71.
24 I.S. Ahuja, J. Inorg. Nucl. Chem., 29 (1967) 2091.
25 E.A. Allen and W. Wilkinson, J. Inorg. Nucl. Chem., 35 (1973) 3135.